

## Article

# Digital Prefabrication of Lightweight Building Elements for Circular Economy: Material-Minimised Ribbed Floor Slabs Made of Extruded Carbon Reinforced Concrete (ExCRC)

Sven Bosbach <sup>1,\*</sup>, Matthias Kalthoff <sup>2</sup>, Cynthia Morales Cruz <sup>3</sup>, Viviane Adam <sup>1</sup>, Thomas Matschei <sup>3</sup>  
and Martin Classen <sup>1</sup>

<sup>1</sup> Institute of Structural Concrete, RWTH Aachen University, 52074 Aachen, Germany

<sup>2</sup> Nessler Bau GmbH, 52076 Aachen, Germany

<sup>3</sup> Institute of Building Materials Research, RWTH Aachen University, 52062 Aachen, Germany

\* Correspondence: sbosbach@imb.rwth-aachen.de

**Abstract:** To reduce resource consumption and the carbon footprint of the construction industry, new construction principles that stipulate the minimisation of materials are urgently needed. Floor slabs show high potential for saving materials and CO<sub>2</sub> emissions, as they account for around 50% of the total volume of concrete used worldwide. A promising approach is the use of corrosion-resistant carbon fibre-reinforced polymer (CFRP) reinforcement, which requires only a small concrete cover to meet bond requirements. Regarding the component's topology, material-efficient ribbed or waffle slabs have been built for decades but their execution has declined owing to their labour-intense production, which calls for manual installation of the formwork. A recently proposed extrusion manufacturing process combines both approaches for material-minimised construction and allows the fast and formwork-free production of carbon reinforced concrete (CRC) components. This article describes the concept, the finding of the form, fabrication and experimental testing of an innovative ribbed floor slab composed of precast extruded carbon reinforced concrete (ExCRC) webs. The novel floor slab consists of a conventionally cast thin-walled top slab and shaped, load-adapted ExCRC webs to achieve high utilisation of the structural member. The ribbed slab provides a lightweight structural system with drastic savings in dead load compared with a conventional steel reinforced slab. In addition, the high durability and service life of the novel floor slabs makes them ideal components to be recovered after an initial life cycle and to be re-used in new construction projects. The paper gives an outlook to the full-scale production of one-way and two-way slab systems made of ExCRC such as ribbed slabs, waffle slabs and sandwich slabs with a honeycomb infill.

**Keywords:** CRC; extrusion; CFRP; material-minimised components; sandwich slab with honeycomb infill; ribbed slab; waffle slab



**Citation:** Bosbach, S.; Kalthoff, M.; Morales Cruz, C.; Adam, V.; Matschei, T.; Classen, M. Digital Prefabrication of Lightweight Building Elements for Circular Economy: Material-Minimised Ribbed Floor Slabs Made of Extruded Carbon Reinforced Concrete (ExCRC). *Buildings* **2023**, *13*, 2928. <https://doi.org/10.3390/buildings13122928>

Academic Editor: Daxu Zhang

Received: 13 October 2023

Revised: 18 November 2023

Accepted: 20 November 2023

Published: 23 November 2023



**Copyright:** © 2023 by the authors. Licensee MDPI, Basel, Switzerland. This article is an open access article distributed under the terms and conditions of the Creative Commons Attribution (CC BY) license (<https://creativecommons.org/licenses/by/4.0/>).

## 1. Introduction

At present, extensive research is being conducted in the area of construction strategies for a circular economy and for materials with a low-carbon footprint, which can be used to manufacture material-minimised components through innovative construction principles [1,2]. One option for reducing the volume of concrete and the related emissions is to substitute steel reinforcement with textile reinforcement made of carbon fibre-reinforced polymer (CFRP). Due to the corrosion resistance of CFRP, textile grids have great potential for use in thin-walled components with high durability [3,4]. These carbon reinforced concrete (CRC) specimens require only a minimum amount of concrete cover to ensure bond requirements [5,6], resulting in slender constructions and a reduction in the amount of concrete [7–10]. This type of material enables the realisation of components that require up to 80% less concrete compared to an equivalent steel reinforced concrete (SRC) member

with an equal load-bearing capacity [11]. The superior ecological performance of thin-walled CRC elements compared to conventional steel reinforced concrete has been shown in [12].

A new serial production method for CRC components is the extrusion process, as presented in [13–15]. Normally, plain concrete elements or fibre-reinforced concrete elements are produced using extrusion processes based on additive manufacturing [16–19]. For decades, extrusion has been established in the field of ceramic materials, e.g., in the production of bricks and stoneware, ceramic catalysts, plastics and concrete spacers. [20,21]. Kalthoff et al. developed a process to introduce prefabricated textile grids into the extrusion process with concrete, thus enabling the production of extruded CRC (ExCRC) with tensile strengths of up to 4000 MPa [15]. The maximum width is currently 60 mm because of the challenging integration of the textiles. The extrusion process is demanding concerning optimisation of the fresh concrete's properties. The concrete has to be extrusion-compatible, but sufficient green strength must be reached once it leaves the mouthpiece in order to obtain the desired geometric shape [16,22].

Another approach is the development of material-efficient components. Innovative concepts for lightweight structures with lower consumption of materials must therefore be developed. An efficient load-adjusted design can be identified, e.g., by optimisation of the topology [23–25] and by exploiting the “form-follows-force” principle [26,27]. In this context, internally nested structures with internal nodes, struts and ties have great potential. In [28], a thin, vaulted concrete ceiling was created using a form-finding and fabrication technique with unique geometries to carry 2.5 times the factored design load in a more critical asymmetric loading scenario. Currently, researchers are concentrating on the development of novel types of modular slab or wall systems, such as those used in [27,29–33], which are intended to minimise the carbon footprint by reducing the material, for example, by using additive manufacturing.

Even decades ago, material-efficient slabs were designed, for example, by Nervi [34], and are currently the focus of renewed research [34,35]. Pier Luigi Nervi designed material-saving slabs whose structure comprises a thin top slab and ribs aligned in the direction of the principal moments, as shown in Figure 1a. In addition, other components have been developed to increase the material-saving potential (Figure 1b). For example, in the case of filigree slabs, approximately 5 cm thick concrete slab elements with the necessary reinforcement are prefabricated in the precast plant and complemented with an in-situ concrete layer after assembly [36]. Alternatively, slab elements can also be prefabricated and assembled on site with grouted joints. For large spans, one-way prestressed precast concrete slabs are an economical solution [37]. The combination of prestressing tendons and voids in the longitudinal direction of the slab in hollow prestressed concrete slabs significantly reduces the dead weight, allowing much larger spans to be realised. A similar weight-minimising approach is applied to biaxially prestressed hollow-core slabs (e.g., Cobiax slabs [38]), which enable significant weight savings through the targeted arrangement of, for example, spherical hollow bodies. In addition to slabs made of reinforced or prestressed concrete slabs, various composite solutions have also been developed (e.g., [39,40]). For example, prefabricated steel profile sheets serve as both the formwork and the tensile element for reinforced concrete slabs produced on site. The bond between concrete and steel is realised by the profiled geometry of the composite sheets or by additional bonding agents. Other composite solutions, such as the Slim-Floor construction method, which combines prefabricated prestressed concrete slabs with steel girders for the bearers, are well established in practice [41].

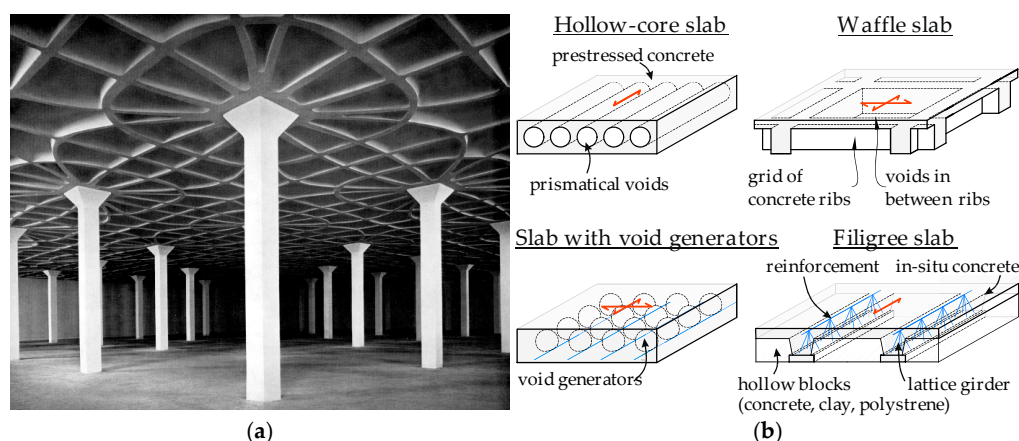


**Figure 1.** (a) Steel-reinforced concrete ribbed slab by Pier Luigi Nervi with webs aligned along the direction of the principal moments [42] (b) and conventional material-efficient slabs [43].

However, the construction of components such as ribbed slabs or waffle slabs requires a high effort of manual labour. Therefore, such structures are rarely used in mass construction in Europe. Recently, research has focused on new perspectives for the construction of such structures [29,43]. Almost all approaches have focused on the use of automated formwork, such as 3D-printed formwork [44] with computerised numerical control (CNC)-milled polystyrene inlays [28] or with printed mineral foam inlays [45], but not yet on the additive manufacturing of the slabs themselves.

An effective method for achieving material-minimised slabs with minimal manual labour and formwork-related effort is to use ribbed slabs with webs made of ExCRC. The arrangement of load-adjusted webs in these slabs allows for a tailored design according to the load path. Novel digitally controlled additive manufacturing processes offer great potential for the minimisation of material, as they allow the individual production of highly complex structural geometries. New variations in the production of material-minimised slabs using ExCRC have recently been demonstrated, as exemplified in [15,46].

This article presents the principal design of the efficient ribbed slabs made of CRC with non-corrosive CFRP grids with minimal use of formwork. In addition, the fabrication of the load-adjusted webs using a laboratory mortar extruder with textiles (LabMorTex) and the assembly process are illustrated. Based on the described design, the feasibility and the performance of the slabs are demonstrated in a demonstrator and tested in a three-point bending test. Finally, the opportunities for the realisation of large-scale material-minimised ceilings using this methodology are presented.

## 2. Materials and Methods

### 2.1. Design of Ribbed Slabs Made of ExCRC

For the implementation of ribbed slabs made from ExCRC, various types of loading for ribbed slabs must be considered. In the first step, both a concentrated load and a distributed load at mid-span was assumed for a one-way slab. It is known that different stress states are induced in the slabs under these two loading conditions. For concentrated loads, the principal moments are aligned, indicating that the webs should be designed with curvature for an optimised arrangement (Figure 2a). For distributed loads, the principal moments are mainly parallel to the longitudinal axis of the slab (Figure 2b).

The implementation of ribbed slabs is not a common solution due to the high formwork effort, although the ribbed slab design is a well-established material-minimising construction method. Therefore, a new method was developed within the scope of this work, which allows the implementation of these ribbed slabs using ExCRC elements. The underlying concepts for the implementation are based on the findings published by the authors in [15,46].

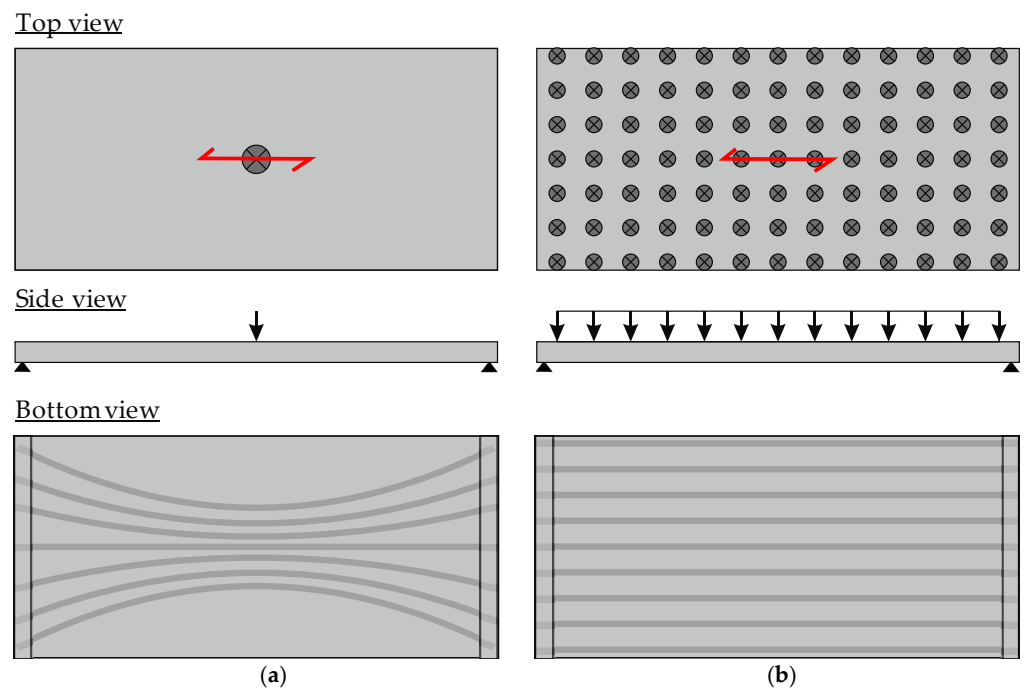


**Figure 2.** Orientation of ExCRC webs in relation to the applied load configuration: (a) concentrated load and (b) distributed load.

The implementation of material-minimised CRC components with ExCRC webs for one-way slabs is shown in Figure 3. The extruded strips are produced as semi-finished products that act as webs within the ceiling structure. To comply with the directions of the principal moments, the strips can be shaped into different radii in the fresh concrete state. The precast webs are then placed in a formwork for casting the thin top slab in an inverted position. Different types of connection can be used to realise cold joining between the extruded CRC webs and the conventionally cast CRC slab.

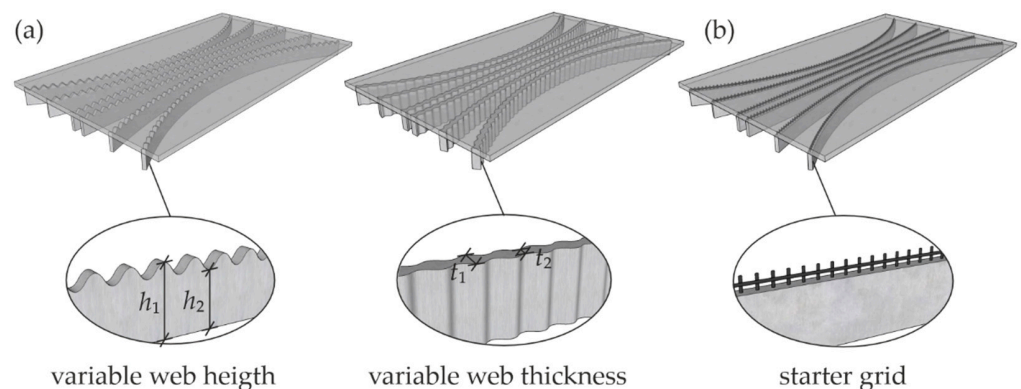


**Figure 3.** Different implementation methods of ExCRC webs: (a) concrete shear connectors and (b) reinforcement connection using starter grids.

The strips can have an undulating cross-section on one side for variable height of the web (Figure 3a). Here, the undulating top surface of the webs is intended to transfer longitudinal shear by interlocking the CRC slab and the ExCRC webs. In addition to vertical undulation (variable height of the webs), it is also possible to produce strips with variable thickness, where the undulating web's surfaces serve as a shear connection (Figure 3b). Alternatively, the connection between the webs and the top slab can be realised using the textile CFRP grids from the webs as starter grids (Figure 3c), which can be realised by only partly integrating the grid during the extrusion process. The shear forces between the top slab and the webs

are then transferred by bond and dowel action. In [47], it was demonstrated that significant dowel forces can also be transferred with textile CFRP reinforcement, which is sensitive to transverse pressure [6]. A combination of all these methods is also possible.

The textile CFRP grids in the webs serve as both flexural and shear reinforcement in the ceiling. By eliminating the need for time-consuming assembly of the formwork, the production costs of the new slab ceiling are significantly reduced compared to conventional production methods, resulting in minimised material costs.

## 2.2. Materials

Two concrete mixtures were used to produce the novel ribbed slab. Mixture 1 is a proven mixture for the extrusion process according to [15]. Mixture 2 is a rheologically optimised mixture used for conventional casting of CRC elements [48,49] with a lower carbon footprint. The composition of the two concretes used, and the compressive and flexural tensile strengths after 28 days, as determined on concrete prisms ( $40 \times 40 \times 160 \text{ mm}^3$ ) according to [50], are given in Table 1. In addition, the intensity of  $\text{CO}_2$  per unit of compressive strength is given for both mixtures.

**Table 1.** Composition of the concretes used.

Parameter	Unit	Extrusion (C1)	Casting (C2)
CEM I 42.5 R		700	-
CEM II/C-M		-	707
Silica fume powder		70	-
Fly ash		210	-
Water		278	165
Sand 2.0–4.0 mm	kg/m <sup>3</sup>	-	596
Sand 1.0–2.0 mm		-	149
Sand 0.5–1.0 mm		-	227
Sand 0.1–0.5 mm		670	220
Sand 0–0.250 mm		-	296
Quartz powder 0–0.250 mm		278	-
Methylcellulose		7.0	-
Superplasticiser	M% of cement	-	1.53
PVA microfibres, $\varnothing/L = 0.026/6 \text{ mm}$	Vol.—%	0.50	-
Compressive strength at 28 d	MPa	65	100
Flexural tensile strength at 28 d		11	11
Intensity of $\text{CO}_2$ per unit of compressive strength	kgCO <sub>2eq</sub> /(m <sup>3</sup> ·MPa)	7.3	3.0

The CFRP grids SITgrid044 KK and Q95-CCE-38-E5 were used as reinforcement. The SITgrid044 KK variant is impregnated with polyacrylate (PA), while the Q95-CCE-21-E5 variant is impregnated with epoxy resin. Pictures of these grids are shown in Figure 4a,b, while the main properties of the grids used are summarised in Table 2.

**Table 2.** Material properties of the CFRP grids used: SITgrid044 VL according to [51] and Q95-CCE-38-E5 according to [47].

Manufacturer's Designation	Impregnation	Tensile Strength <sup>1</sup>	Young's Modulus <sup>1</sup>	Mesh Size <sup>1</sup>	Cross-Section <sup>1</sup>
		[MPa]	[GPa]	[mm]	[mm <sup>2</sup> /m]
SITgrid044 KK	PA	2000/1840	150/150	12	35.3
Q95-CCE-38-E5	Epoxy resin	3710/3490	231/244	38	95.0

<sup>1</sup> Warp and weft direction.

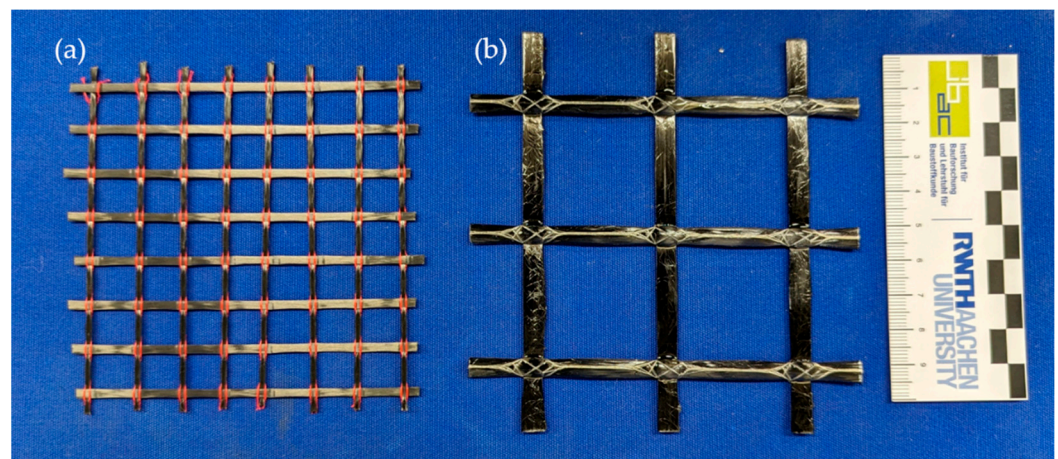


**Figure 4.** (a) CFRP grid SITgrid044 KK by Wilhem Kneits GmbH, Wirsberg, Germany and (b) CFRP grid Q95-CCE-38-E5 by Solidian GmbH, Albstadt, Germany.

### 3. Laboratory-Scale Implementation of a One-Way ExCRC Slab

#### 3.1. Design Selection

In order to demonstrate the feasibility of ribbed slabs with load-adjusted webs made of ExCRC, a one-way slab demonstrator for a concentrated load at mid-span was selected and designed. The design of the demonstrator and the orientation of the webs are shown in Figure 5.

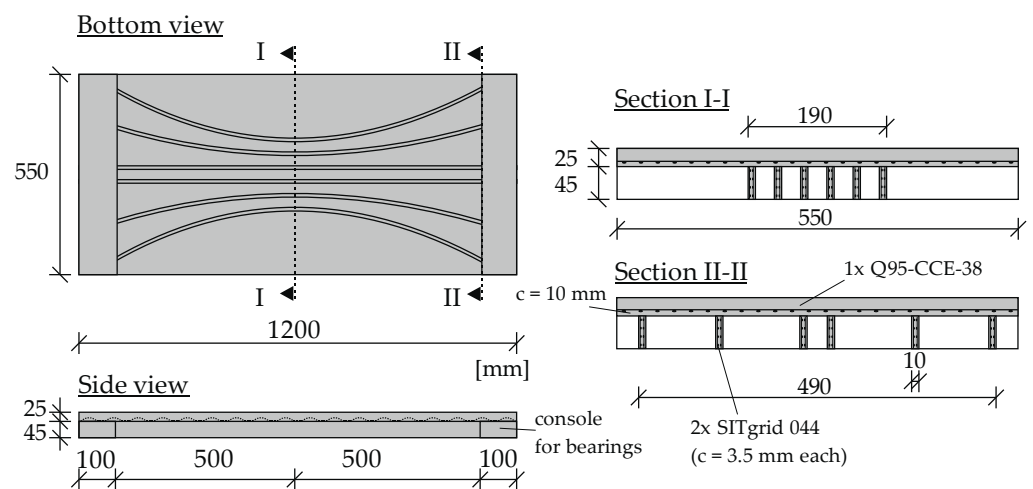


**Figure 5.** Design of the demonstrator and web orientation of the ExCRC slab for a concentrated load at mid-span.

Due to the given production dimensions of the extruder (LabMorTex), the maximum width of the ExCRC strips was limited to only 60 mm. Therefore, a scaled demonstrator with a total ceiling depth of 70 mm was designed. The height of the webs (without undulations for cold-joint connection) was 45 mm, and the top slab had a thickness of 25 mm. The slab's length was chosen to be 1.2 m, while the slab's width was set to 0.55 m. The load-adjusted ExCRC webs featured different radii of 0, 60 and 120 cm for an efficient load transfer within the slab. These load-adjusted webs enhanced the flexural capacity. In a ribbed slab with straight webs, only the webs in the centre of the slab are typically activated for a concentrated load, with a load distribution of  $45^\circ$  according to [52]. As a result, not all webs are fully involved in the load transfer, resulting in reduced flexural capacity.

### 3.2. Production of the Concrete

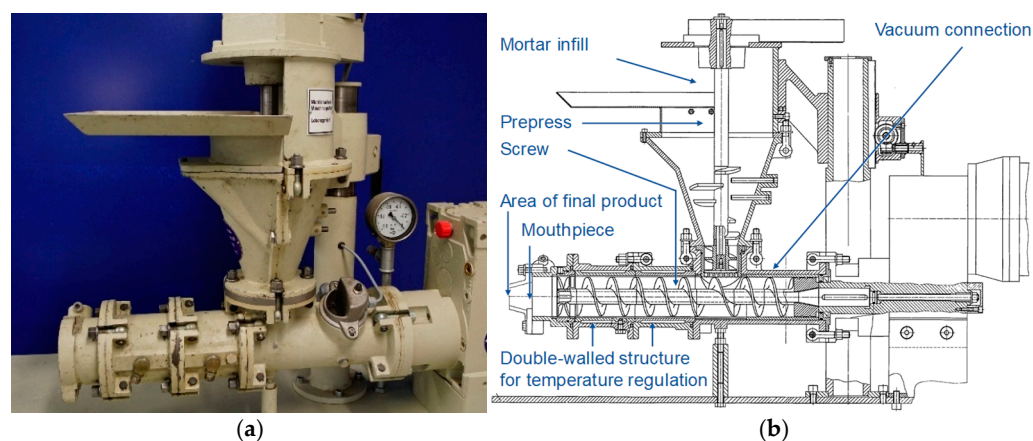
As in the studies in [13–15,22,51,53], an Eirich R05T intensive mixer, with a maximum capacity of 40 L, was used for the production of the concrete (Mixture C1, Table 1) for the extrusion process. For improved control of the process during batching, the engine's data, the mixer's temperature and the resistance torque were monitored during the mixing procedures. Each batch produced 18 L of fresh concrete. Initially, the dry components were homogenised at 500 revolutions per minute for one minute. Water was then added within 15 s at 66 revolutions per minute. Afterwards, the concrete was mixed for a further 130 s at 800 revolutions per minute. Eventually, the revolutions per minute were gradually decreased by 100 revolutions every 15 s to examine the rheological behaviour of the mixtures at different loads.

Concrete Mixture C2 was prepared in a compulsory mixer for the casting of the slab. All dry ingredients were first homogenised for 1 min, then the water and superplasticiser were added and mixed for a further 5–6 min. The resulting concrete was then poured into the formwork.

### 3.3. Concrete Extrusion Process

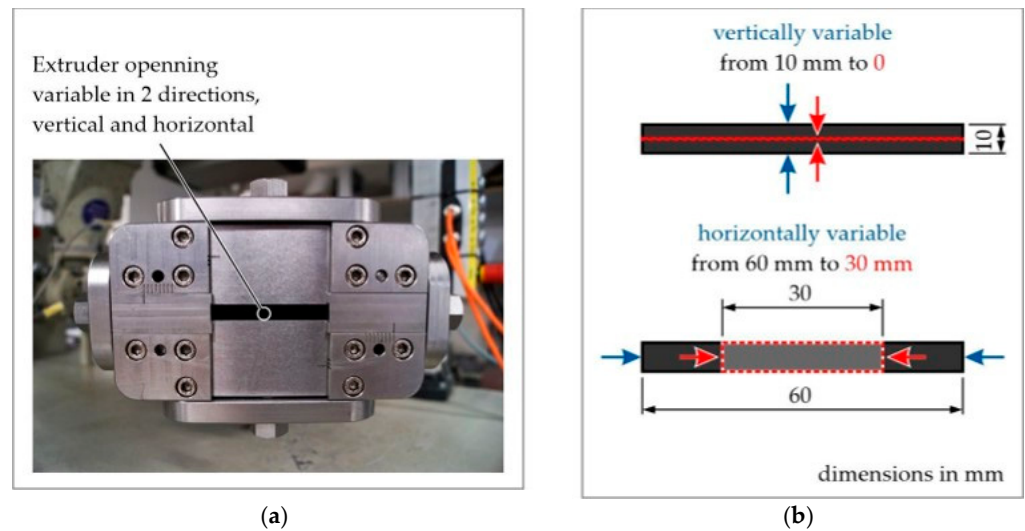
A Händle laboratory extruder was used for the extrusion of the undulating ExCRC webs. The extrusion process of the laboratory extruder (LabMorTex) has already been presented in detail in [15,51]. Therefore, the procedure is just briefly described here. The extruder consists of a prepress and a screw. At the end of the auger, different mouthpieces with different geometries can be attached. It is also possible to create a vacuum in the transition area between the prepress and the main auger, which removes air and compresses the extrudate.

Figure 6a shows the laboratory extruder, and Figure 6b depicts a technical drawing of the extruder. Within the scope of this work, a new mouthpiece was used to produce the extruded CRC webs. This mouthpiece allows the extrusion of concrete with two textile layers and a variable cross-section [46]. The textiles were inserted horizontally into the mouthpiece and then transported out of it with the concrete.



**Figure 6.** (a) Extruder (LabMorTex) [51]. (b) Technical drawing of the LabMorTex [51].

The wavy cross-section required for the interlocked connection between the webs and the top slab was realised by using an innovative variable mouthpiece as described in [54]. Steel plates were located on all sides of the mouthpiece to allow horizontal and vertical adjustment of the cross-section. The precise positioning of these plates within the mouthpiece was controlled by screws. As a result, the width of the extruded specimen could be varied between 30 and 60 mm, and the height can be adjusted between 0 and 10 mm. The mouthpiece is illustrated in Figure 7a.



**Figure 7.** (a) Close-up of the variable mouthpiece and (b) a schematic representation of the possible cross-sectional variations without reinforcement [54].

In this study, only the width was adjusted between 45 and 60 mm. Therefore, stepper motors with speeds of up to 3000 rpm were used to screw the plates into position. The motors could be controlled remotely, allowing the cross-section and speed to be adjusted. A framework was designed to align and transmit motion from the motors to the adjustment screws, enabling horizontal and vertical positioning. The motors and framework are shown in Figure 7b.

During production, the grids were first cut to the desired curved geometry of the webs and then inserted into the extruder through the mouthpiece, where the grids were then extruded together with the concrete. After leaving the mouthpiece, the ExCRC strips, each measuring approximately 1200 mm long, were transported on a conveyor belt and immediately positioned on a negative mould. The negative moulds had the previously determined bending radii described in Section 3.1 [13]. The three calculated bending radii of 0, 60 and 120 cm were achieved with a deviation of 3–4 cm. The concrete cover between the textiles and the concrete surface was approximately 3 mm.

### 3.4. Assembly of the Demonstrator

For manufacturing the slab, the ExCRC webs were assembled into the top slab. Placement of the precast ExCRC strips can be achieved either manually or by an industrial robot. A cast-in-place formwork was used to cast the top slab upside down (Figure 8a). In addition, one layer of the Q95-CCE-38-E5 grid was positioned within the top slab using plastic-based spacers from Solidian GmbH (concrete cover  $c = 10$  mm), which served as a support structure for the ExCRC webs. Concrete C2 (cf. Table 1) was then mixed and poured into the formwork until the webs were embedded in the formwork by 15 mm. The casted slab is shown in Figure 8b.



**Figure 8.** Manufacturing and assembly of the demonstrator: (a) ExCRC web assembled on grid of top slab and (b) completed ribbed slab.

To support the assembled slab in the 3-point bending test, additional supports were casted from concrete C2 at both ends of the slab. All webs were embedded in these supports. After one day of hardening, the formwork was removed and the ribbed slab was rotated, thus being prepared for further transportation.

### 3.5. Testing of the Demonstrator

The structural performance of the small-scale ribbed slab was tested in a 3-point bending test with a concentrated load at mid-span, which was applied deformation controlled at 0.1 mm/min. The span was defined to 110 cm. The test setup is shown in Figure 9.

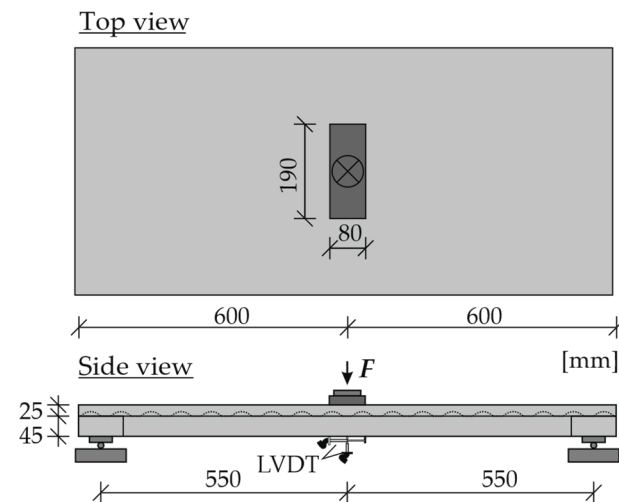


**Figure 9.** Schematic representation of the three-point-bending test setup.

Two roller bearings were used for the supports, and the concentrated load was applied by a rigid steel plate with a conical/spherical steel bearing to prevent imperfections. During the test, the applied load and displacement of the cylinder were measured, together with the vertical displacement at mid-span in three sections. In addition, the cracks in the webs were recorded during the test using two cameras positioned beneath the ceiling.

## 4. Results and Discussion

### 4.1. Test Results

The demonstrator slab failed in bending with a maximum flexural capacity of 1.57 kNm. Figure 10a shows the vertical displacement at mid-span measured by the three LVDTs. After an initial stiff, uncracked phase up to an applied bending moment of 0.81 kNm, multiple cracking occurred, with reduced stiffness. After a displacement of approximately 19 mm, the lowest yarns in the middle webs failed in tension, resulting in a significant load drop. As a result, the slab had a sufficient announcement of failure ( $w_{\max} = l/58$ ), which is particularly important for components made from brittle materials such as HPC and CFRP reinforcements. A small increase in the deflection and load was measured, followed by a further load drop as more yarns failed in tension. Subsequently, the test was stopped to record the crack pattern of the slab.

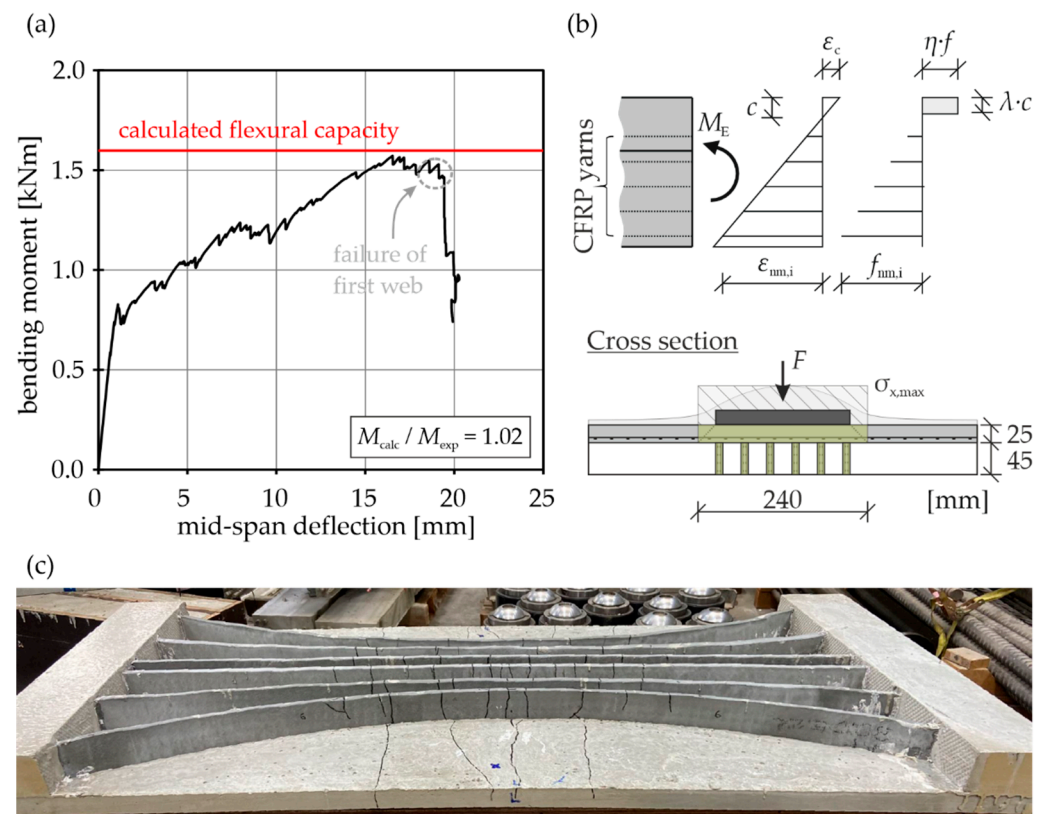


**Figure 10.** (a) Moment–deflection relationship, (b) iterative design of flexural capacity and (c) crack pattern at the bottom side of the ribbed slab after failure.

The flexural capacity can also be calculated by an iterative design, taking into account all longitudinal yarns in the webs and the yarns in the tensile zone of the top slab, following the flexural design of simple prismatic CRC members presented in, for example, [55,56]. Consequently, a rectangular stress block and only the effective width of the top slab at mid-span were considered for the calculation. For the chosen single load in the demonstrator test, all six webs were loaded, resulting in the effective cross-section shown in Figure 10b, with the total effective width of the top slab being 240 mm. The flexural capacity  $M_{calc}$  could therefore be calculated according to Equation (1).

$$M_{calc} = \sum \sigma_{nm,i} \cdot A_{nm,i} \cdot z_{nm,i} \quad (1)$$

where  $\sigma_{nm,i}$  is the stress in the individual yarns,  $A_{nm,i}$  is the yarns' cross-section in each reinforcement layer and  $z_{nm,i}$  is the distance between the reinforcement layers and the center of the rectangular stress block. The flexural capacity is obtained when the yarns' tensile strength  $f_{nm}$  is reached in the lowest yarns. As shown in Figure 10a, the flexural capacity could be accurately calculated using an iterative design ( $M_{calc}/M_{exp} = 1.02$ ).

Figure 10c shows the crack pattern of the slab demonstrator after failure at the bottom side. All webs were activated, and the cracks propagated into the top slab. There was no evidence of cracking or slipping in the joint between the top slab and the webs, demonstrating that the variable surface of the ExCRC webs was sufficient to provide interlocking between the top slab and the webs. The inclined shear cracks occurred after flexural failure. Thus, sufficient activation of the whole slab could be assumed.

The results show that, for the first time, a ribbed slab made of ExCRC elements was successfully implemented on a small scale. The efficient extrusion process was developed to enable the extrusion of ExCRC with variable cross-sections. Due to their high green strength, the variable ExCRC strips could also be formed to the desired bending radius immediately after extrusion. This process can significantly simplify the production of ribbed

and waffle slabs compared to other manufacturing techniques used for material-minimised slabs (e.g., [29,31]).

#### 4.2. Upscaling for Real-Scale Applications

The application of the demonstrator showed the potential for realising ribbed slabs made of ExCRC. To upscale the small-scale demonstrator to full-scale applications and to increase the flexural capacity, a further increase in the webs' height is foreseen in future studies. Simply doubling the webs' height to 120 mm could result in a 373% increase in flexural strength ( $M_{\max}$  ( $h_{\text{web}} = 120 \text{ mm}$ ) = 6 kNm) according to the iterative design method of [55,56]. However, this requires a modification of the extruder's mouthpiece. The implementation of such a mouthpiece is expensive but technically feasible. Additional investigation concerning the optimisation of the rheological behaviour of the extruded concrete are necessary and are currently subject of investigation. To further increase the load-bearing capacity of the slab, high-strength reinforcements with tensile strengths of approximately 4000 MPa could be used instead of the SITgrid044 KK reinforcement in the webs, as successfully demonstrated in [15,46].

For the connection between the ExCRC webs and the top slab, it is conceivable to use textile CFRP reinforcement as starter bars or grids. In this case, a part of the reinforcement would protrude uncovered during extrusion, serving as the connection to the slab (cf. Section 2.1). With this type of slab, up to 80% of the concrete could be saved compared with a conventional steel reinforced concrete slab with the same flexural strength [46]. However, larger deflections and higher shear stresses between the top slab and webs are expected. Further investigation at the joints is thus required.

Optionally, a bottom CRC facing can also be implemented using ExCRC webs with top and bottom starter grids. Additional flexural reinforcement can be implemented into this CRC facing, which leads to significantly increased flexural capacity of such sandwich slabs. The use of an additional bottom CRC facing in sandwich slabs also improves the fire resistance and acoustic insulation (Figure 11a).

For the production of two-way slabs made with ExCRC webs, the implementation of different types of formed webs (shown in Figure 11b) is conceivable. Therefore, the ExCRC strips are first extruded as described in Section 3.3. The ExCRC strips are then formed into a variety of possible geometries. For example, the ExCRC webs may follow the direction of the principal moments within the two-way slab. Therefore, the strips are shaped with different radii. Once the shaped ExCRC strips have hardened, they were assembled as shown in Figure 11b and inserted into the fresh concrete of a cast CRC facing (the top slab). Optionally, an additional bottom slab with flexural reinforcement could significantly increase the flexural capacity.

Alternatively, the extruded strips could be formed into corrugated webs. Through placement of these webs close to each other, a sandwich slab with a honeycomb core, which is commonly used in sandwich components (e.g., [57–59]), can be realised, allowing for load transfer in two directions of the ceiling. These floor slabs have an additional bottom CRC layer for the integration of longitudinal flexural reinforcement. Through this, the corrugated webs forming the honeycomb structure are only activated for transferring shear forces by strut-and-tie action, while the tensile forces from global bending are carried by the straight flexural reinforcement in the bottom slab. This design minimises out-of-plane bending of the corrugated webs and significantly increases the efficient use of the CFRP reinforcement.

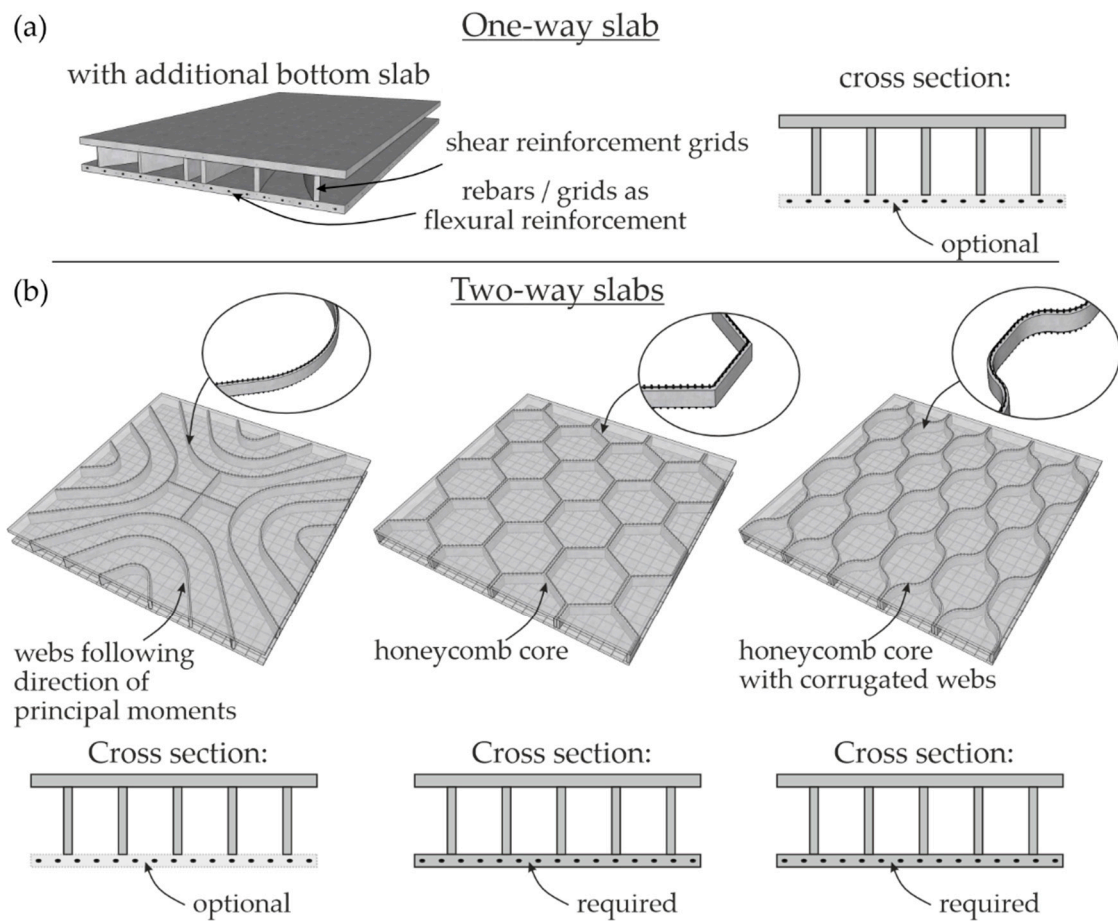


**Figure 11.** (a) Ribbed slab made of ExCRC for one-way slabs with an additional bottom slab and (b) sandwich slabs with different infills made of ExCRC for two-way slabs.

To further automate the process, robots will be used to insert the extruded strips into the moulds on a factory scale, allowing the highly efficient production of ribbed and waffle slabs. To demonstrate the general manufacturing process, Figure 12 illustrates the process using the example of a biaxial sandwich slab with a honeycomb infill. First, the bottom slab is classically reinforced with a biaxial CFRP grid (1). The robot then inserts the prefabricated ExCRC webs, for example, with starter grids, into the formwork on top of the grid, ensuring sufficient concrete cover and a friction-locked connection between the webs and the bottom slab (2 and 3). In order to be able to place the webs directly on the reinforcement, a rigid grid is chosen, for example, impregnated with epoxy resin, which is dimensionally stable and eliminates the need for additional spacers. After casting or 3D printing of the bottom slab and curing of the concrete (4), the entire ceiling is rotated (5) to cast the top slab (6 and 7) to create the finished ceiling with a honeycomb core.

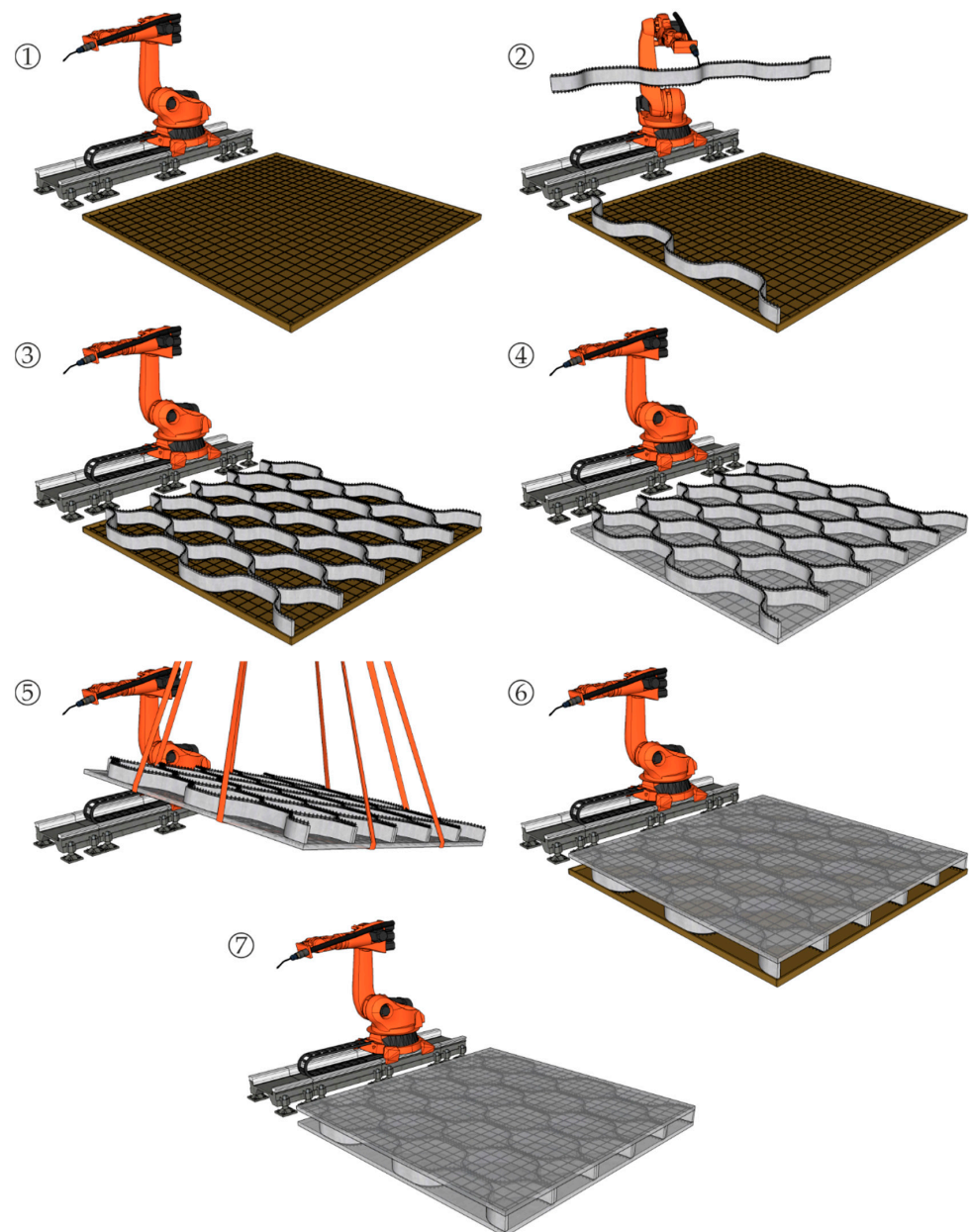


**Figure 12.** Manufacturing process of a biaxial sandwich slab with a honeycomb infill.

## 5. Conclusions

This publication presented the design of an innovative ribbed slab demonstrator, which was implemented using extruded CRC components and tested in a three-point bending test. The webs were manufactured using an innovative mouthpiece that allowed the extrusion of double-layered reinforced CRC strips with variable cross-sections. Immediately after extrusion, the variable CRC strips were specifically shaped into different radii according to the principal moments resulting from a single load at mid-span applied in the demonstration test. A thin CRC slab was then cast, and the variable extruded CRC strips were embedded in the fresh concrete. The main findings presented in this article can be summarised as follows:

- For the first time, an innovative ribbed slab with load-adjusted webs was designed and implemented using extruded variably shaped CRC strips with two layers of textile CFRP grids and a conventionally cast CRC top slab.

- The method developed here allows the production of ExCRC web components with a variable cross-section that can be automatically incorporated into ribbed slabs. The easy and formwork-free production allows very economic realisation compared with conventionally cast ribbed slabs.
- Testing of the ExCRC slab demonstrator showed the sufficient strength of the joints between the slab and the webs, resulting in flexural failure of the webs. The flexural capacity of the tested ExCRC slab demonstrator could be accurately estimated by a simple iterative calculation.
- Based on the test results, the technical requirements for the implementation of the innovative ribbed slab made of ExCRC on a plant scale for one-way and two-way slabs were demonstrated.
- The addition of a bottom concrete layer for the integration of longitudinal reinforcement and the use of corrugated extruded CRC webs for the realisation of a honeycomb core for the ceiling are important measures to further increase efficiency.

Further research will investigate the upscaling of the ribbed slab and the implementation of biaxially loaded slabs with a honeycomb core according to the approach presented in Section 4.2. For both uniaxial and biaxial slabs, large-scale tests will be conducted for an investigation of the structural behaviour. In addition, the connection between the CRC slab and the ExCRC webs will be investigated in detail, taking other joining principles into account.

**Author Contributions:** Conceptualisation, S.B., M.K., C.M.C. and M.C.; methodology, S.B., M.K., C.M.C. and M.C.; software, S.B., M.K. and C.M.C.; validation, S.B., M.K. and C.M.C.; investigation, S.B., M.K. and C.M.C.; resources, T.M. and M.C.; data curation, S.B., M.K. and C.M.C.; writing—original draft preparation, S.B., M.K. and C.M.C.; writing—review and editing, V.A., T.M. and M.C.; visualisation, S.B., M.K. and C.M.C.; supervision, T.M. and M.C.; project administration, T.M. and M.C.; funding acquisition, T.M. and M.C. All authors have read and agreed to the published version of the manuscript.

**Funding:** This research was funded by the Deutsche Forschungsgemeinschaft (DFG, German Research Foundation) SFB/TRR 280 (project ID: 417002380).

**Data Availability Statement:** The data presented in this study are available on request from the corresponding authors.

**Acknowledgments:** Funded by the Deutsche Forschungsgemeinschaft (DFG, German Research Foundation) SFB/TRR 280 (project ID: 417002380). The authors would like to thank the DFG for supporting the research project.

**Conflicts of Interest:** Author Matthias Kalthoff was employed by the company nesslerer bau GmbH. The remaining authors declare that the research was conducted in the absence of any commercial or financial relationships that could be construed as a potential conflict of interest.

## References

1. Beckmann, B.; Bielak, J.; Bosbach, S.; Scheerer, S.; Schmidt, C.; Hegger, J.; Curbach, M. Collaborative research on carbon reinforced concrete structures in the CRC/TRR 280 project. *Civ. Eng. Des.* **2021**, *3*, 99–109. [\[CrossRef\]](#)
2. Janani, R.; Lalithambigai, N. A critical literature review on minimization of material wastes in construction projects. *Mater. Today Proc.* **2021**, *37*, 3061–3065. [\[CrossRef\]](#)
3. Spelter, A.; Bergmann, S.; Bielak, J.; Hegger, J. Long-Term Durability of Carbon-Reinforced Concrete: An Overview and Experimental Investigations. *Appl. Sci.* **2019**, *9*, 1651. [\[CrossRef\]](#)
4. Tietze, M.; Kirmse, S.; Kahnt, A.; Schladitz, F.; Curbach, M. The ecological and economic advantages of carbon reinforced concrete—Using the C 3 result house CUBE especially the BOX value chain as an example. *Civ. Eng. Des.* **2022**, *4*, 79–88. [\[CrossRef\]](#)
5. Bielak, J.; Spelter, A.; Will, N.; Claßen, M. Verankerungsverhalten textiler Bewehrungen in dünnen Betonbauteilen. *BUST* **2018**, *113*, 515–524. [\[CrossRef\]](#)
6. Stark, A.; Classen, M.; Hegger, J. Bond behaviour of CFRP tendons in UHPFRC. *Eng. Struct.* **2019**, *178*, 148–161. [\[CrossRef\]](#)
7. Morales Cruz, C. Crack-Distributing Carbon Textile Reinforced Concrete Protection Layers. Ph.D. Thesis, RWTH Aachen University, Aachen, Germany, 2020. [\[CrossRef\]](#)

8. Zhang, M.; Deng, M. Tensile behavior of textile-reinforced composites made of highly ductile fiber-reinforced concrete and carbon textiles. *J. Build. Eng.* **2022**, *57*, 104824. [[CrossRef](#)]
9. Bielak, J.; Schöneberg, J.; Classen, M.; Hegger, J. Shear capacity of continuous concrete slabs with CFRP reinforcement. *Constr. Build. Mater.* **2022**, *320*, 126117. [[CrossRef](#)]
10. Liao, J.; Lin, X.-C.; Zhu, D.-H.; Zheng, Y.; Zeng, J.-J.; Ma, C.-L.; Zhao, H.-C. Behavior of FRP grid-reinforced ultra-high performance concrete (UHPC) pipes under lateral compression. *Case Stud. Constr. Mater.* **2023**, *19*, e02189. [[CrossRef](#)]
11. Schladitz, F. Carbonbeton—Was ist schon möglich? Aktueller Stand der Entwicklung und Forschung. *Beton Fachz. Bau Tech.* **2019**, *69*, 156–161.
12. Backes, J.G.; Schmidt, L.; Bielak, J.; Del Rosario, P.; Traverso, M.; Claßen, M. Comparative Cradle-to-Grave Carbon Footprint of a CFRP-Grid Reinforced Concrete Façade Panel. *Sustainability* **2023**, *15*, 11548. [[CrossRef](#)]
13. Kalthoff, M.; Raupach, M.; Matschei, T. Extrusion and Subsequent Transformation of Textile-Reinforced Mortar Components—Requirements on the Textile, Mortar and Process Parameters with a Laboratory Mortar Extruder (LabMorTex). *Buildings* **2022**, *12*, 726. [[CrossRef](#)]
14. Kalthoff, M.; Bosbach, S.; Matschei, T.; Raupach, M.; Claßen, M.; Hegger, J. Investigations on material-minimized slabs made of extruded carbon reinforced concrete. In Proceedings of the Fib International Congress 2022, Oslo, Norway, 12–16 June 2022.
15. Kalthoff, M. Extruded Thin-Walled Textile Reinforced Concrete Components with Flexible Shape. Ph.D. Thesis, RWTH Aachen University, Aachen, Germany, 2023. [[CrossRef](#)]
16. Alfani, R.; Guerrini, G.L. Rheological test methods for the characterization of extrudable cement-based materials—A review. *Mat. Struct.* **2005**, *38*, 239–247. [[CrossRef](#)]
17. Perrot, A.; Rangeard, D.; Nerella, V.N.; Mechtcherine, V. Extrusion of cement-based materials—An overview. *RILEM Tech. Lett.* **2018**, *3*, 91–97. [[CrossRef](#)]
18. Zhou, X.; Li, Z. Manufacturing cement-based materials and building products via extrusion: From laboratory to factory. *Proc. Inst. Civ. Eng. Civ. Eng.* **2015**, *168*, 11–16. [[CrossRef](#)]
19. Meurer, M.; Classen, M. Mechanical Properties of Hardened 3D Printed Concretes and Mortars-Development of a Consistent Experimental Characterization Strategy. *Materials* **2021**, *14*, 752. [[CrossRef](#)]
20. Händle, F. (Ed.) *The Art of Ceramic Extrusion*, 1st ed.; Springer International Publishing; Springer: Cham, Switzerland, 2019; ISBN 978-3-030-05254-6.
21. Beeckman, J.W.L. *Catalyst Engineering Technology: Fundamentals and Applications*; Wiley: Hoboken, NJ, USA, 2020; ISBN 9781119634942.
22. Kalthoff, M.; Raupach, M.; Matschei, T. Investigation of Rheological Test Methods for the Suitability of Mortars for Manufacturing of Textile-Reinforced Concrete Using a Laboratory Mortar Extruder (LabMorTex). *Constr. Mater.* **2022**, *2*, 217–233. [[CrossRef](#)]
23. Lewis, W. Form-Finding Approach to Modelling Minimal Structural Forms, with Analogy to Nature. In *Proceedings ISSA 2016: Innovative Structural Systems in Architecture, 3–5 November 2016, Wroclaw, Poland*; Wroclaw Branch of the Polish Academy of Sciences: Wroclaw, Poland, 2016; pp. 39–42.
24. Lewis, W.J. Tension cables in suspension bridges. A case of form-finding. In *Tension Structures: Form and Behaviour*, 2nd ed.; Lewis, W.J., Ed.; ICE Publishing: Leeds, UK, 2017; pp. 101–133. ISBN 978-0-7277-6173-6. [[CrossRef](#)]
25. Smarslik, M.; Ahrens, M.A.; Mark, P. Toward holistic tension- or compression-biased structural designs using topology optimization. *Eng. Struct.* **2019**, *199*, 109632. [[CrossRef](#)]
26. Hegger, J.; Herbrand, M.; Stark, A.; Classen, M. Betonbau der Zukunft: Leicht, filigran und nachhaltig. *Bauing* **2015**, *90*, 337–344. [[CrossRef](#)]
27. Stark, A.; Classen, M.; Knorrek, C.; Camps, B.; Hegger, J. Sandwich panels with folded plate and doubly curved UHPFRC facings. *Struct. Concr.* **2018**, *19*, 1851–1861. [[CrossRef](#)]
28. Liew, A.; López, D.L.; van Mele, T.; Block, P. Design, fabrication and testing of a prototype, thin-vaulted, unreinforced concrete floor. *Eng. Struct.* **2017**, *137*, 323–335. [[CrossRef](#)]
29. Mata-Falcón, J.; Bischof, P.; Huber, T.; Anton, A.; Burger, J.; Ranaudo, F.; Jipa, A.; Gebhard, L.; Reiter, L.; Lloret-Fritschi, E.; et al. Digitally fabricated ribbed concrete floor slabs: A sustainable solution for construction. *RILEM Tech. Lett.* **2022**, *7*, 68–78. [[CrossRef](#)]
30. Jayasinghe, A.; Orr, J.; Hawkins, W.; Ibell, T.; Boshoff, W.P. Comparing different strategies of minimising embodied carbon in concrete floors. *J. Clean. Prod.* **2022**, *345*, 131177. [[CrossRef](#)]
31. Rippmann, M.; Liew, A.; van Mele, T.; Block, P. Design, fabrication and testing of discrete 3D sand-printed floor prototypes. *Mater. Today Commun.* **2018**, *15*, 254–259. [[CrossRef](#)]
32. Antony, F.; Griefhammer, R.; Speck, T.; Speck, O. Sustainability assessment of a lightweight biomimetic ceiling structure. *Bioinspir. Biomim.* **2014**, *9*, 16013. [[CrossRef](#)]
33. Classen, M.; Dressen, T. Experimental Investigations on Prestressed Concrete Beams with Openings. *ACI Struct. J.* **2015**, *112*, 221. [[CrossRef](#)]
34. Halpern, A.B.; Billington, D.P.; Adriaenssens, S. The ribbed floor slab systems of pier luigi nervi. *J. IASS* **2013**, *54*, 127–136.
35. Rempel, S.; Will, N.; Hegger, J.; Beul, P. Filigrane Bauwerke aus Textilbeton. *Beton Stahlbetonbau* **2015**, *110*, 83–93. [[CrossRef](#)]
36. Furche, J.; Bauermeister, U. *Beton-Kalender 2016: Schwerpunkte: Beton im Hochbau, Silos und Behälter*, 1st ed.; Ernst Wilhelm & Sohn: Berlin, Germany, 2015; ISBN 978-3-433-03074-5.

37. Roggendorf, T.; Hegger, J. Zur Querkrafttragfähigkeit von Spannbeton-Fertigdecken bei biegeweicher Lagerung—Teil 1: Modellentwicklung. *Beton Stahlbetonbau* **2011**, *106*, 531–539. [[CrossRef](#)]
38. Abramski, M.; Albert, A.; Pfeffer, K.; Schnell, J. Experimentelle und numerische Untersuchungen zum Tragverhalten von Stahlbetondecken mit kugelförmigen Hohlkörpern. *Beton Stahlbetonbau* **2010**, *105*, 349–361. [[CrossRef](#)]
39. Ackermann, F.P. Load-Bearing Behaviour of Steel Fibre Reinforced Continuous Composite Slabs. Ph.D. Thesis, Technische Universität Kaiserslautern, Kaiserslautern, Germany, 2010. ISBN 9783941438484.
40. Hegger, J.; Claßen, M.; Schaumann, P.; Sothmann, J.; Feldmann, M.; Döring, B. Entwicklung einer integrierten Verbunddecke für nachhaltige Stahlbauten. *Stahlbau* **2013**, *82*, 11–17. [[CrossRef](#)]
41. Hegger, J.; Kerkeni, N.; Roggendorf, T. Zum Tragverhalten von Slim-Floor-Konstruktionen. *Beton- Stahlbetonbau Sonderdr. Flachdecken* **2008**, *1*, 5–14. [[CrossRef](#)]
42. Nervi, P.L.; Rogers, E.N.; Joedicke, J.P. *Bauten und Projekte*; Gerd Hatje: Stuttgart, Germany, 1957.
43. Huber, T.; Burger, J.; Mata-Falcón, J.; Kaufmann, W. Structural design and testing of material optimized ribbed RC slabs with 3D printed formwork. *Struct. Concr.* **2023**, *24*, 1932–1955. [[CrossRef](#)]
44. Hansemann, G.; Schmid, R.; Holzinger, C.; Tapley, J.; Kim, H.H.; Sliskovic, V.; Freytag, B.; Trummer, A.; Peters, S. Additive fabrication of concrete elements by robots: Lightweight concrete ceiling. In *Fabricate 2020: Making Resilient Architecture*; Burry, J., Sabin, J., Sheil, B., Skavara, M., Eds.; UCL Press: London, UK, 2020.
45. Bedarf, P.; Szabo, A.; Zanini, M.; Heusi, A.; Dillenburger, B. Robotic 3D printing of mineral foam for a lightweight composite concrete slab. In Proceedings of the 26th International Conference of the Association for Computer-Aided Architectural Design Research in Asia (CAADRIA 2021), Hong Kong, China, 29 March–1 April 2021; Association for Computer-Aided Architectural Design Research in Asia (CAADRIA): Hong Kong, China, 2022; pp. 61–70.
46. Kalthoff, M.; Bosbach, S.; Backes, J.G.; Morales Cruz, C.; Claßen, M.; Traverso, M.; Raupach, M.; Matschei, T. Fabrication of lightweight, carbon textile reinforced concrete components with internally nested lattice structure using 2-layer extrusion by LabMorTex. *Constr. Build. Mater.* **2023**, *395*, 132334. [[CrossRef](#)]
47. Bosbach, S.; Hegger, J.; Claßen, M. Dowel action of CFRP shear reinforcement in carbon reinforced concrete: (under review). *Constr. Build. Mater.* **2023**.
48. Bielak, J. Shear in Slabs with Non-Metallic Reinforcement. Ph.D. Thesis, RWTH Aachen University, Aachen, Germany, 2021. [[CrossRef](#)]
49. Schneider, K.; Butler, M.; Mechtcherine, V. Carbon Concrete Composites C 3—Nachhaltige Bindemittel und Betone für die Zukunft. *Beton Stahlbetonbau* **2017**, *112*, 784–794. [[CrossRef](#)]
50. *DIN EN 196-1:2016-11*; Methods of Testing Cement—Part 1: Determination of Strength. German Version EN 196-1:2016. Beuth Verlag GmbH: Berlin, Germany, 2016. [[CrossRef](#)]
51. Kalthoff, M.; Raupach, M.; Matschei, T. Investigation into the Integration of Impregnated Glass and Carbon Textiles in a Laboratory Mortar Extruder (LabMorTex). *Materials* **2021**, *14*, 7406. [[CrossRef](#)]
52. *DAfStb-Heft 240*; Deutscher Ausschuss für Stahlbeton. Ernst & Sohn: Hoboken, NJ, USA, 1991.
53. Kalthoff, M.; Raupach, M.; Matschei, T. Materialminimiertes Bauen mit extrudiertem Textilbeton. *Beton* **2022**, *72*, 195–198.
54. Beckers, J.; Kalthoff, M.; Morales Cruz, C.; Matschei, T. Possibilities of extrusion production in concrete construction. In *Beiträge zur 10. DAfStb-Jahrestagung mit 62. Forschungskolloquium 26–27. September 2023*; Hegger, J., Claßen, M., Raupach, M., Matschei, T., Schmidt, M., Alvarez y Leal, A., Eds.; RWTH Aachen University: Aachen, Germany, 2023; pp. 161–169. [[CrossRef](#)]
55. Rempel, S.; Ricker, M.; Hegger, J. Biegebemessungsmodell mit einer geschlossenen und iterativen Lösung für Textilbetonbauteile. *Beton Stahlbetonbau* **2020**, *115*, 218–230. [[CrossRef](#)]
56. Preinstorfer, P.; Kromoser, B.; Kollegger, J. Flexural behaviour of filigree slab elements made of carbon reinforced UHPC. *Constr. Build. Mater.* **2019**, *199*, 416–423. [[CrossRef](#)]
57. Papila, M.; Atilgan, A.R. All-composite honeycomb core sandwich structures: Master curves for stiffness-based design. *Forces Mech.* **2022**, *6*, 100066. [[CrossRef](#)]
58. Goswami, S. On the Prediction of Effective Material Properties of Cellular Hexagonal Honeycomb Core. *J. Reinf. Plast. Compos.* **2006**, *25*, 393–405. [[CrossRef](#)]
59. Ghanbari-Ghazijahani, T.; Kasebahadi, M.; Hassanli, R.; Classen, M. 3D printed honeycomb cellular beams made of composite materials (plastic and timber). *Constr. Build. Mater.* **2022**, *315*, 125541. [[CrossRef](#)]

**Disclaimer/Publisher’s Note:** The statements, opinions and data contained in all publications are solely those of the individual author(s) and contributor(s) and not of MDPI and/or the editor(s). MDPI and/or the editor(s) disclaim responsibility for any injury to people or property resulting from any ideas, methods, instructions or products referred to in the content.